Published in final edited form as:

Free Radic Biol Med. 2016 December ; 101: 10–19. doi:10.1016/j.freeradbiomed.2016.09.021.

4-Hydroxynonenal dependent alteration of TRPV1-mediated coronary microvascular signaling

Daniel J. DelloStritto[a], **Pritam Sinharoy**[c], **Patrick J. Connell**[a], **Joseph N. Fahmy**[a], **Holly C. Cappelli**[a,b], **Charles K. Thodeti**[a], **Werner J. Geldenhuys**[d], **Derek S. Damron**[c], and **Ian N. Bratz**[a]

[a]Department of Integrative Medical Sciences, Northeast Ohio Medical University, 4209 St. Rt. 44, Rootstown, OH 44272, USA

[b]Department of Biomedical Sciences, Kent State University, 256 Cunningham Hall, Kent, OH 44242, USA

[c]Department of Biological Sciences, Kent State University, 256 Cunningham Hall, Kent, OH 44242, USA

[d]Department of Pharmaceutical Sciences, School of Pharmacy, West Virginia University, P.O. Box 9500, Morgantown, WV 26506, USA

Abstract

We demonstrated previously that TRPV1-dependent regulation of coronary blood flow (CBF) is disrupted in diabetes. Further, we have shown that endothelial TRPV1 is differentially regulated, ultimately leading to the inactivation of TRPV1, when exposed to a prolonged pathophysiological oxidative environment. This environment has been shown to increase lipid peroxidation byproducts including 4-Hydroxynonenal (4-HNE). 4-HNE is notorious for producing protein post-translation modification (PTM) via reactions with the amino acids: cysteine, histidine and lysine. Thus, we sought to determine if 4-HNE mediated post-translational modification of TRPV1 could account for dysfunctional TRPV1-mediated signaling observed in diabetes. Our initial studies demonstrate 4-HNE infusion decreases TRPV1-dependent coronary blood flow in C57BKS/J (WT) mice. Further, we found that TRPV1-dependent vasorelaxation was suppressed after 4-HNE treatment in isolated mouse coronary arterioles. Moreover, we demonstrate 4-HNE significantly inhibited TRPV1 currents and Ca^{2+} entry utilizing patch-clamp electrophysiology and calcium imaging respectively. Using molecular modeling, we identified potential pore cysteines residues that, when mutated, could restore TRPV1 function in the presence of 4-HNE. Specifically, complete rescue of capsaicin-mediated activation of TRPV1 was obtained following mutation of pore Cysteine 621. Finally, His tag pull-down of TRPV1 in HEK cells treated with 4-HNE demonstrated a significant increase in 4-HNE binding to TRPV1, which was reduced in the TRPV1 C621G mutant. Taken together these data suggest that 4-HNE decreases TRPV1-mediated responses, at both the in vivo and in vitro levels and this dysfunction can be rescued via mutation of the pore Cysteine 621. Our results show the first evidence of an amino acid specific

Correspondence to: Ian N. Bratz.

Conflict of interest

None declared.

modification of TRPV1 by 4-HNE suggesting this 4-HNE-dependent modification of TRPV1 may contribute to microvascular dysfunction and tissue perfusion deficits characteristic of diabetes.

Keywords

TRPV1; 4-Hydroxynonenal; Coronary regulation; Lipid peroxidation; Post-translational modification; Reactive oxygen species

1. Introduction

Diabetes is a rapidly growing epidemic resulting in increased morbidity and mortality due to vascular disease [1,2]. Microvascular dysfunction is a phenomenon known to occur at higher incidences in diabetic patients likely leading to the observed increase in mortality [3]. Previous work from our laboratory has demonstrated an attenuated contribution of Transient Receptor Potential Vanilloid 1 (TRPV1) channels to microvascular regulation in coronary arteries in a murine model of diabetes (db/db mice) [4]. TRPV1, originally discovered as a receptor for nociception, is a polymodal cation channel that preferentially conducts Ca^{2+} for initiating intracellular signaling cascades [5–7] which has been found to be expressed in numerous tissues including the vasculature [8,9]. We and others have shown that TRPV1 plays a role in the cardiovascular system, including the regulation of blood pressure and coronary blood flow (CBF) [10–12].

Reactive Oxygen Species (ROS) are important for proper homeostasis of numerous biological functions, including cellular events ranging from apoptosis to inflammation to host-defense reactions [13]. However, when an imbalance in ROS exists, as in diabetes, many deleterious cellular consequences occur often leading to altered protein, DNA and lipid function. Aberrant ROS can lead to dysfunctional activity in the cell. One such consequence of aberrant ROS levels is the non-enzymatic peroxidation of lipids [14], leading to the generation of α,β-unsaturated aldehydes including 4-Hydroxynonenal (4-HNE), 4-oxynonenal (4-ONE) and 4-hydroxy-2-hexenal (4-HHE), which are generated from the peroxidation of ω-6 or ω-3-polyunsaturated fatty acids. 4-HNE, one of the most abundant and potent reactive carbonyl species [15], is known to react with the thiol group on cysteine residues (including modification of histidine and lysine residues), leading to the formation of covalent adducts and resulting in protein post-translational modification (PTM) [16–18]. Importantly, 4-HNE-mediated modification has been shown to alter protein function including, protein activation, signaling disruption and decreased expression [19–22].

TRPV1 has recently been identified as a broad sensor of oxidative stress, a phenomenon which has been characterized in other TRP channels as well [23,24]. This unique nature of TRPV1, sensitivity to oxidative stimuli and regulation of vascular function, led us to investigate the consequence of TRPV1 covalent modification on vascular function. Having recently demonstrated that an enhanced oxidative environment (i.e. diabetic state) diminishes TRPV1 activity [25], the aim of our current study was to investigate the role of 4-HNE on TRPV1-mediated vascular signaling. Moreover, we aimed to further explore the physical interaction and PTM of TRPV1 by 4-HNE. We hypothesize that 4-HNE-mediated

PTM elicits TRPV1 dysfunction via covalent cysteine modification, and that mutation of such cysteines can completely rescue the function of TRPV1. Further, we predict this modification would lead to decreased TRPV1-mediated vasoreactivity of the coronary arterials, potentially contributing to microvascular dysfunction and the resultant perfusion impairments observed in diabetes.

2. Methods and materials

2.1. Mice

All procedures were conducted with the approval of the Institutional Animal Care and Use Committee of the Northeast Ohio Medical University (NEOMED) and in accordance with National Institutes of Health *Guidelines for the Care and Use of Laboratory Animals* (NIH publication 2011). Breeding pairs of mice were originally purchased from Jackson Labs (Bar Harbor, ME) after which mice were bred in the NEOMED animal facility. Experiments were performed in 10–12 week-old male C57BKS/J (WT) mice and db/db mice. Mice were housed in a temperature-controlled room with a 12:12-h light-dark cycle and maintained with access to food and water ad libitum.

2.2. Jugular and femoral artery catheterization

Mice received a surgical plane of inhaled anesthesia (1.5–2.5% sevoflurane). Mice were secured in the supine position and placed under a dissecting microscope with temperature control at 37 °C. The right jugular vein was visualized and cannulated for intravenous drug infusions. See Methods and Materials Section from DelloStritto et al., for complete description [25].

2.3. Contrast echocardiography CBF measurements

For myocardial contrast echocardiography (MCE), animals were prepared as mentioned above. Mice were infused with capsaicin (1–100 μg/kg), 4-HNE (4 mg/kg over 10 min), and non-targeted contrast. For complete description of methods, see Guarini et al. [4] and DelloStritto et al. [25].

2.4. Experimental protocol

Following the completion of jugular canulation surgery, mice were given a bolus injection of the ganglionic blocker hexamethonium (HEX, 5 mg/kg, Sigma) to eliminate reflex adjustments and focus on the primary vascular actions of capsaicin. Initial studies were performed to determine the effects of continuous infusion of capsaicin administered in an escalating fashion, at a rate of 20 μl/min for 4 min. In the presence and absence of 4-HNE, pressure and heart rate was continuously recorded.

2.5. Isolated coronary microvessel reactivity studies

Briefly, mice were anesthetized, upon which hearts were excised, and placed in ice-cold physiological saline solution. Coronary arterioles were dissected free from ventricular wall tissue, in buffer containing (mM): 145 NaCl, 5.0 KCl, 2.5 $CaCl_2$, 1.17 $MgSO_4$, 25.0 $NaHCO_3$, 10 glucose; pH 7.4. Arterioles were pressurized to 60 mmHg and warmed to

37 °C. Vessel viability was determined using 60 mM KCl. Vessels were pre-contracted with the thromboxane mimetic, U46619 (1 μM) and relaxation to capsaicin was observed. Effects of 4-HNE on capsaicin-mediated relaxation were performed following 1-h intraluminal infusion of 4-HNE (10 μM).

2.6. Molecular modeling and docking studies

Molecular modeling studies were performed using YASARA 14.7.17 (www.yasara.org) [26]. The crystal structure of TRPV1 was used in our studies [6,27]. The structure of 4-HNE was obtained from PubChem and used in the docking studies with TRPV1. Using the docking program, Autodock VINA [28], which is integrated into YASARA, global docking to the protein was assessed and binding simulations were then visually inspected for feasible interactions.

2.7. Cell culture and transient transfection

Human Embryonic Kidney-293A (HEK293) cells were maintained in Dulbecco's Modified Eagle's Media (ThermoFisher, Carlsbad, CA) supplemented with 10% Fetal Bovine Serum, 2 mM L-Glutamine, 100 U/mL Penicillin and 100 μg/mL Streptomycin. Commercially available murine coronary endothelial cells (MCECs) (Cell Biologics, Chicago, Il) were maintained (from passages 1–6) in mouse endothelial cell basal media provided. HEK293 cells were plated in a 12-well plate for 24–48 h, after which, the cells were transfected utilizing Mirus TransIT®-2020 according to the manufactures protocol. pCDNA3-Rat TRPV1(WT) (gift from Dr. David Julius), pCDNA3-Rat TRPV1(C616G, C621G, C634G and Tri-C mutant) (gift from Dr. Viktorie Vlakova) were co-transfected with EGFP-N1 (Clontech) (4:1 ratio). Cells were used within 36–48 h following transfection.

2.8. Cell survival assay

To examine the effects of 4-HNE treatment on cell survival, a PrestoBlue® assay (measure of cell survival) was performed on HEK following prolonged 4-HNE treatment (1-h) at concentrations ranging from 1 μM to 2 mM. Briefly, HEK cells were seeded into a 96-well plate and allowed to grow to confluence. Cells were treated with 4-HNE in complete media (1 μM to 2 mM) for 1-h. Following the 1-h treatment, the combination of 4-HNE and media was removed and cells were washed with PBS. PrestoBlue® reagent (Invitrogen, Carlsbad, CA) was added to complete media and subsequently added to each well. Following a 4-h incubation, plates were read for fluorescence (535 nm excitation/615 nm emission) according to manufacturers' protocol. Each treatment was done in triplicate and data represents 3 separate experiments.

2.9. Patch-clamp electrophysiology

TRPV1-dependent currents were examined by whole-cell patch clamp recordings at room temperature in transfected HEK cells. Data were acquired and analyzed using an Axopatch 200B amplifier and pCLAMP10 software (Axon Instruments, Union City, CA, USA). Currents were filtered with a low pass Bessel filter at 1 kHz and sampled at 5 kHz. Borosilicate pipettes (Sutter, Novato, CA, USA) were polished to resistances of 2–5 MΩ. I–V relations were obtained as previously described [8]. Extracellular bath solution contained

(in mM) 135 NaCl, 5 KCl, 2CaCl2, 1 MgCl2, 10 Glucose, 10 HEPES 5 Tris-base, and pH 7.4 with NaOH. Intracellular solutions contained (in mM) 140 KCl 1 MgCl2, 1 EGTA, 5 MgATP, 1 Na-GTP, 10 HEPES, 5 Tris-base, and pH 7.1 with KOH.

2.10. Intracellular calcium imaging

MCECs were initially treated for 1 h with 4-HNE (10 μM), a concentration known to be representative of pathophysiological levels [29], and then incubated at 37 °C for 30 min with fura-2 acetoxy methylester (fura-2/AM; 2 μmol/L) in endothelial cell media without FBS (Cell Biologics). Cells were grown on glass cover slides and subsequently mounted onto an Olympus IX-81 inverted fluorescence microscope (Olympus America, Lake Success, NY) and visualized. Drugs were perfused in at a rate of 2 mL/min. For more details, see Materials Methods from Zhang et. al [30]. Cells were analyzed for peak differences in calcium-influx vs. baseline. For both Patch-Clamp and Ca^{2+}-imaging, solutions containing 4-HNE (basal buffer) and capsaicin (treatment buffer) were kept separate to prevent any potential interaction between the two compounds.

2.11. 4-HNE PTM quantification

HEK293 cells were cultured and transfected with WT and C621G plasmids contain respective mutants. Following 48-h incubation, cells were treated with 10 μM 4-HNE for 1 h. Cells were then washed with ice cold PBS and Triton-X 100 Buffer (without EDTA), containing proteinase cocktail inhibitor, (Sigma Aldrich, St. Louis, MO), was added to each sample for protein isolation. Following incubation, cells were centrifuged at 20,000×*g* for 20 min and supernatant was collected. Dynabeads® with a Ni-NTA moiety was added to the supernatant, following manufacturers' instructions (ThermoFischer, Carlsbad, CA). Samples were allowed to sit for 10 min at 4 °C with 20 mM imidazole to reduce non-specific binding. The samples were then washed with 50 mM sodium-phosphate buffer, pH 8.0, 300 mM NaCl, 0.01% Tween-20 and 50 mM imidazole. Following the final wash, beads were mixed with 300 mM imidazole, 50 mM sodium-phosphate buffer, pH 8.0, 300 mM NaCl and 0.01% Tween-20, to elute the protein of interest. Samples were reduced utilizing laemlli buffer and then loaded into an acrylamide gel. Samples were then transferred to PVDF membrane and blocked with milk/TBST. Goat anti-4-HNE antibody (Millipore, Darmstadt, Germany) was initially used to probe 4-HNE PTM with appropriate secondary for visualization. To verify total TRPV1 protein expression, the same membrane was stripped and reprobed with rabbit anti-TRPV1 (Santa Cruz Biotechnology, Santa Cruz, CA, USA). Membranes were washed with excess TBST and rabbit anti-goat secondary (Santa Cruz Biotechnology, Santa Cruz, CA, USA) was utilized for 4-HNE primary and goat anti-rabbit secondary (Santa Cruz Biotechnology, Santa Cruz, CA, USA) was utilized for TRPV1 primary.

2.12. Drugs

All drugs were purchased from Sigma Chemicals (St. Louis, MO, USA) unless otherwise stated. Capsaicin was dissolved in stock solutions of ethanol. Hexamethonium (5 mg/mL) stock solution was made up in saline. 4-HNE was purchased from Caymen Chemical at stock solution of 10 mg/mL in ethanol.

2.13. Statistics

Data are expressed as mean ± SEM. Statistical comparisons were made with paired *t*-tests, one-way or two-way repeated measures analysis of variance (ANOVA; with Bonferroni multiple comparison) as appropriate. For statistical analyses, GraphPad Prism 6.0 software for Windows 7 (GraphPad Software, San Diego, Calif) was utilized. In all tests, $P < 0.05$ was considered statistically significant.

3. Results

3.1. 4-HNE blunts capsaicin-mediated increases in CBF and coronary relaxation

Initial studies investigated the influence of 4-HNE on TRPV1-mediated CBF regulation. Capsaicin (given intrajugularly (IJ); 1–100 μg/kg/min) mediated changes in CBF in WT mice were blunted at 10 and 20 μg/kg/min concentrations following prior administration of 4-HNE (IJ; 4 mg/kg over 10 min) administration (Fig. 1A). No effects of capsaicin on blood pressure and heart rate (continually monitored) were observed (Table 1). Using isolated murine coronary microvessels, 4-HNE effects on capsaicin-mediated relaxation were examined before and following intraluminal infusion of 4-HNE (10 μM) for 1-h. 4-HNE markedly attenuated capsaicin-mediated relaxation (Fig. 1B). Similarly, 4-HNE treatment had no further effect on capsaicin-mediated vasorelaxation in isolated microvessels from db/db mice (Fig. 1C).

3.2. 4-HNE decreases TRPV1 currents and calcium influx

We next examined if 4-HNE attenuates TRPV1-mediated current using patch-clamp electrophysiology. Using HEK293 cells transiently transfected with pCDNA3-TRPV1 (WT), cells were treated with 4-HNE (10 μM) for 1-h, isolated, and TRPV1-specific currents were examined while cells remained in 4-HNE supplemented media. 4-HNE treatment significantly decreased TRPV1 activity to 100 nM capsaicin (Fig. 2A). Cell survivability was examined via PrestoBlue® assay, which verified that this observed decrease in activity was not due to increased cellular death (Fig. 2B). Moreover, the sodium nitroprusside and acetylcholine-dependent relaxation were examined to determine the specificity of 4-HNE on capsaicin-mediated relaxation. Importantly, 4-HNE had no effect on ACh or SNP-dependent mechanisms of relaxation (Supplemental Fig. 1).

Calcium imaging of fura-2 acetoxy methylester (fura-2/AM; 2 μmol/L) loaded MCECs on capsaicin-mediated calcium influx was used to further verify the effect of 4-HNE treatment (10 μM for 1 h) on intrinsic TRPV1 activity. Representative traces demonstrate capsaicin-mediated transient increases in intracellular free Ca^{2+} concentration ($[Ca^{2+}]_i$) (Fig. 3A), which were significantly blunted following 4-HNE treatment (Fig. 3B and D). To confirm the specificity of capsaicin activation, cells pretreated with the TRPV1 antagonist SB366791 (10 μM) demonstrated a complete lack of capsaicin-mediated transient increases in $[Ca^{2+}]_i$. (Fig. 3C). Similar to the electrophysiology results, prolonged 4-HNE treatment significantly diminished capsaicin-dependent increases in $[Ca^{2+}]_i$ in MCECs (Fig. 3D).

3.3. Pore-forming cysteine residues responsible for apparent 4-HNE-induced decreased TRPV1 activity

Using the in silico modeling program YASARA 14.7.17 (www.yasara.org), we initially explored potential 4-HNE covalent modification sites. Following the construction of the 6 transmembrane subunit of TRPV1 using YASARA 14.7.17, potential interactions between 4-HNE and TRPV1 were examined using binding algorithms inherent to the program (Autodock VINA). Autodock VINA revealed that 4-HNE has multiple potential binding motifs on TRPV1 (Fig. 4), in particular centered around cysteine residues in the pore helices (TM5-TM6), specifically Cysteine residues 616, 621 and 634. Using the same binding algorithms, the effects of a single point residue mutation (cysteine to glycine) on 4-HNE-mediated PTM. Importantly, the single point mutations for each individual residue (C616C, C621G or C634G) or in concert (TriC) had no effect on the overall predicted structure of TRPV1, yet Autodock VINA predicted a decrease in 4-HNE-mediated PTM on TRPV1 pore residues (Fig. 4C–F).

Plasmids pertaining to the four specific mutations were transfected into HEK cells and exposed to capsaicin to initially examine channel functionality. Capsaicin-dependent TRPV1 currents in the four mutant constructs (C616G, C621G, C634G and TriC) showed no statistical significant difference compared to the WT-TRPV1 construct (Fig. 5A–D). Having established attenuated 4-HNE-mediated PTM on TRPV1 pore residues using computational mapping and binding algorithms, we next assessed each mutant construct's ability to rescue TRPV1 function when exposed to prolonged 4-HNE treatment (10 μM for 1 h). Patch-clamp analysis of the TriC mutant construct revealed its ability to rescue capsaicin-induced TRPV1 currents in the presence of 4-HNE (Fig. 6D). To further elucidate the specific residue(s) vital to restoration of channel activity, each individual mutant construct was examined in the presence of 4-HNE. Interestingly, C616G and C634G displayed attenuated capsaicin-mediated currents similar to the WT-TRPV1 construct in the presence of 4-HNE (Fig. 6A and C); whereas, the mutant construct C621G, exhibited complete rescue similar to the TriC mutant (Fig. 6B).

3.4. Direct 4-HNE binding to TRPV1

To further validate that 4-HNE mediated decreases in TRPV1 activity was due to modification of residue C621, 6× His-tag pull-downs were performed on HEK293 cells transfected with WT and C621G mutant constructs containing 6× His-tag. Following 36–48 h post transfection, cells were treated with 10 μM 4-HNE for 1 h and TRPV1 was pulled down using a Ni-NTA moiety (Dynabeads) and then probed for 4-HNE covalent modification. We found significant interaction between WT-TRPV1 and 4-HNE compared to the vehicle cells (~1.3-fold increase) (Fig. 7A and B). However, this 4-HNE-TRPV1 interaction was significantly reduced in cells expressing C621G-TRPV1 mutant (Fig. 7A and C) (note: the first lane of the representative blot is from a separate experiment compared to latter lanes). These data suggest 4-HNE modifies residue C621 to alter its channel activity as evidenced by our electrophysiology results.

4. Discussion

Our present study demonstrates that 4-HNE directly affects TRPV1 activity, as demonstrated on a vertical scale from the cellular level to the in vivo regulation of coronary blood flow. Furthermore, we illustrate a key pore cysteine residue, cysteine 621, is responsible for the impaired activity associated with 4-HNE binding. In addition, we establish a role for the pore forming cysteine residues in the regulation of TRPV1 function, specifically as a target for 4-HNE-mediated PTM. Finally, we found that single amino acid mutation could rescue TRPV1 function in the presence of 4-HNE. Taken together, our results establish a novel role of 4-HNE modification of TRPV1 to elicit decreased channel activity, which ultimately could contribute to aberrant microvascular dysfunction and regulation of CBF observed in diabetes.

The production of 4-HNE is a well-established phenomenon resulting from the imbalance of oxidative stress. In the case of diabetic patients, reports have demonstrated an increase in 4-HNE modification levels compared to non-diabetic patients [31,32]. Furthermore, 4-HNE has also been demonstrated to play a critical role in cardiovascular diseases, specifically, in the development and progression of atherosclerosis, cardiac hypertrophy and myocardial ischemia-reperfusion [33,34]. In spontaneously hypertensive rats, 4-HNE levels were increased leading to adduct formation with liver kinase B1 (LKB1) [35]. Formation of this adduct reduced the activity of LKB1, leading to an increase activity of mTOR/p706S kinase in isolated cardiomyocytes resulting in a hypertrophy [35]. Recently, our lab has demonstrated a reduced capacity of TRPV1-dependent regulation of CBF in diabetes [4]. Further evidence demonstrates that TRPV1 is differentially regulated under conditions of oxidative stress. As such, acute H_2O_2 exposure activates TRPV1, eliciting a vascular response (relaxation), but if an increased oxidative environment (or exposure) persists, it leads to decreased TRPV1 activity [25]. This decrease in activity was similar to that observed in the current study following 4-HNE exposure. A natural progression of elevated ROS (either exposure and/or levels) in diabetes is associated with increased lipid peroxidation, which could further explain our previous findings [25]. However, we cannot discount two (or more) separate pathways altering TRPV1 activity, whereby an increase in ROS (specifically H_2O_2) leads to altered cysteine function. This modification of cysteine could be accomplished via reversible oxidation (sulfenylation) or potentially irreversible modification such as the formation of a side group of sulfinic or sulfonic acid [36].

The reactivity and/or selectivity of 4-HNE's to each amino acid is quite different, as it is known to preferentially modify cysteine residues (0.6 M HNE/amino acids ratio) over histidine (1×10^{-3}) and lysine (3×10^{-4}) residues [16,37]. Due to their reactive nature, adduct formation with proteins, phospholipids and nucleic acids has been linked to cytotoxic events [14,32]. Indeed, harmful levels of 4-HNE have been associated with enhanced protein degradation and inhibition of protein function, specifically related to kinases, membrane proteins and ion channels [19,38,39]. Furthermore, 4-HNE has been shown to play a direct role in the vasculature in many respects. Its role in atherosclerosis is important as a prominent event in the increase levels of oxidized LDL particles infiltrating the vascular smooth muscle cell (VSMC) layer [33]. This leads to increased stress signaling and proliferation within the VSMC [40]. In addition, plaque formation increases when

endothelial function becomes impaired and 4-HNE has also been observed to contribute to said endothelial dysfunction. In an elegant study by Usatyuk et. al., the authors demonstrated 4-HNE-dependent disruption of the endothelial barrier resulting from 4-HNE-mediated increases in ROS production. Using trans-endothelial electrical resistance measurements, the authors demonstrated 4-HNE treatment disrupted the endothelial barrier through aberrant MAPK signaling cascade (specifically ERK, JNK, and p38 MAPK) resulting in actin remodeling [41]. Interestingly, the authors demonstrated a differential effect of 4-HNE such that at lower concentrations (< 50 μM), this effect was independent of cell death and apoptosis; however, at higher and longer treatments cell death was apparent. Subsequent studies also investigated the importance of glutathione pools. Specifically noting that prevention of increased endothelial permeability was accomplished pharmacologically by rescuing glutathione pools with NAC and mercaptopropionyl glycine [38].

Oxidative stress-mediated regulation of ion channels has been of recent interest by many groups. TRP channels, specifically TRPV1 and TRPA1, have become well recognized as broad sensors of oxidative challenges [42]. Chuang et. el. demonstrated the sensitivity of TRPV1 to reactive oxygen species, specifically H_2O_2 [43], identifying the importance of cysteine modification in TRPV1 activity. Further work by Susankova et. al. demonstrated key pore cysteines are sensitive to dithiothreitol relative to TRPV1's temperature sensitivity and activation [44]. A recent study reported the ability of 4-HNE to interact and activate the TRPA1 channel [42]. In that same study, 4-HNE-mediated activation of TRPV1 was examined and shown to have no effect on channel activation. Similarly, Kishimoto et al., recently demonstrated the possibility of 4-HNE-dependent modification of TRPV1 [in esophageal cells], although no direct effects on channel activity were examined [9]. The TRPV1 structure/sequence reveals that there are 19 cysteines residues per subunit, with only a few known to be redox sensitive, specifically the 3 pore region cysteines of interest in the current study. Recently, David Julius' lab elucidated a partial structure for TRPV1 with high-resolution Cryo-EM [6,7]. With further exploration of this structure in multiple states, this advancement in the field will bring about greater understanding of ion channels, including the exploration of how PTM (including 4-HNE) affects ion channel gating, kinetics and/or structure.

Understanding oxidative challenges to TRPV1, specifically endothelial TRPV1, will lead to further insights into the regulation of vascular function. In the current study, we demonstrate that oxidative stress-induced PTM (4-HNE) of TRPV1 was associated with attenuated endothelial TRPV1 signaling. Furthermore, the effects of 4-HNE on the vasculature are illustrated through the alteration of endothelial nitric oxide (NO) production. Pope et. al. demonstrated 4-HNE decreases NO release through decreased activity of dimethylarginine dimethylamine hydrolase (DDAH), a protein involved in methylarginine metabolism [45]. This regulation of NO production by eNOS is complex and multifactorial with the integration and balance between competing signals and even the physical interaction between other proteins, such as caveolin-1 [46,47]. While our study does not directly investigate the role of TRPV1 and eNOS, previous studies from our lab and others have investigated this integral relationship [4,48–50]. Specifically, it has been demonstrated that TRPV1 activation, results in Ca^{2+} mobilization, leading to eNOS-mediated NO production via an AKT-CaMKII-AMPK signaling pathway. Overall, this suggests a convergence of

pathways that when disrupted contribute to endothelial and microvascular dysfunction observed in diabetes.

Overall, the current study provides novel insight into physiological consequences of 4-HNE aberrant regulation of ion channels and the functional importance of pore cysteine residues in TRPV1. A diverse combination of the lipid peroxidation products have been demonstrated to increase in diabetes and alter cellular functions [29,51]. However, 4-HNE is the most widely studied as it is derived from ω-6-polyunsaturated fats formed via non-enzymatic processes [29,51]. Although not directly examined, we cannot exclude the possibility of other lipid peroxidation products from contributing to the altered function of TRPV1 seen in diabetes. Future studies will examine the role for other lipid peroxidation products on TRPV1 function. Finally, TRPV1 possesses 19 cysteine residues in one subunit of its tetrameric structure with each cysteine possessing a unique microenvironment susceptible to a variety of stimuli [52,53]. Interestingly, the lack of 4-HNE to completely block TRPV1 response to 4-HNE (as noted in Figs. 2 and 6) demonstrates that either the concentration of 4-HNE was not sufficient to render this action or other cysteine residues outside the pore region are modified by 4-HNE. Moreover, in Fig. 4C–F when the pore cysteine residues are mutated and the binding algorithm is rerun, an observed shift in 4-HNE modulation to localization around other cysteine residues is noted. Although the current manuscript demonstrates a likely role for C621 in the 4-HNE dependent blunting of endothelial TRPV1 signaling, the ability of 4-HNE to PTM other residues (cysteine, histidine and lysine) to effect TRPV1 signaling cannot be discounted. Future studies will address these concerns.

In conclusion, this study demonstrates the ability of 4-HNE dependent PTM to attenuate TRPV1-dependent signaling, vascular function and regulation of CBF. 4-HNE is responsible for decreased TRPV1 activity via apparent PTM of the Cysteine 621 residue in the pore forming region. The functional consequence of 4-HNE–associated PTM of TRPV1 results in decreased TRPV1-dependent endothelial signaling ultimately contributing to microvascular dysfunction.

Supplementary Material

Refer to Web version on PubMed Central for supplementary material.

Acknowledgments

Funding

This study was supported by start-up funds provided by NEOMED (IB), 15PRE24470072 from the American Heart Association (DJD), and NIH R01HL119705 (CKT).

We would like to thank Matthew Kiedrowski for his guidance in the molecular biology specifically in the creation of the His-tagged moieties on WT and C621G TRPV1.

References

1. Danaei G, Finucane MM, Lu Y, Singh GM, Cowan MJ, Paciorek CJ, Lin JK, Farzadfar F, Khang YH, Stevens GA, Rao M, Ali MK, Riley LM, Robinson CA, Ezzati M. National, regional, and global trends in fasting plasma glucose and diabetes prevalence since 1980: systematic analysis of

health examination surveys and epidemiological studies with 370 country-years and 2·7 million participants. Lancet. 2011; 378:31–40. [PubMed: 21705069]

2. CDC. Increasing prevalence of diagnosed diabetes – United States and Puerto Rico, 1995–2010. MMWR. Morbidity and mortality weekly report. 2012; 61:918–921. [PubMed: 23151951]
3. Joshi M, Kotha SR, Malireddy S, Selvaraju V, Satoskar AR, Palesty A, McFadden DW, Parinandi NL, Maulik N. Conundrum of pathogenesis of diabetic cardiomyopathy: role of vascular endothelial dysfunction, reactive oxygen species, and mitochondria. Mol Cell Biochem. 2014; 386:233–249. [PubMed: 24307101]
4. Guarini G, Ohanyan VA, Kmetz JG, DelloStritto DJ, Thoppil RJ, Thodeti CK, Meszaros JG, Damron DS, Bratz IN. Disruption of TRPV1-mediated coupling of coronary blood flow to cardiac metabolism in diabetic mice: role of nitric oxide and BK channels. Am J Physiol – Heart Circ Physiol. 2012; 303:H216–H223. [PubMed: 22610171]
5. Caterina MJ, Schumacher MA, Tominaga M, Rosen TA, Levine JD, Julius D. The capsaicin receptor: a heat-activated ion channel in the pain pathway. Nature. 1997; 389:816–824. [PubMed: 9349813]
6. Liao M, Cao D, Julius ED, Cheng Y. Structure of the TRPV1 ion channel determined by electron cryo-microscopy. Nature. 2013
7. Cao E, Liao Y, Cheng M, Cheng Y, Julius D. TRPV1 structures in distinct conformations reveal activation mechanisms. Nature. 2013
8. Bratz IN, Dick GM, Tune JD, Edwards JM, Neeb ZP, Dincer UD, Sturek M. Impaired capsaicin-induced relaxation of coronary arteries in a porcine model of the metabolic syndrome. Am J Physiol – Heart Circ Physiol. 2008; 294:H2489–H2496. [PubMed: 18390821]
9. Kishimoto E, Naito Y, Handa O, Okada H, Mizushima K, Hirai Y, Nakabe N, Uchiyama K, Ishikawa T, Takagi T, Yagi N, Kokura S, Yoshida N, Yoshikawa T. Oxidative stress-induced posttranslational modification of TRPV1 expressed in esophageal epithelial cells. Am J Physiol – Gastrointest Liver Physiol. 2011; 301:G230–G238. [PubMed: 21636531]
10. Inoue R, Jensen LJ, Shi J, Morita H, Nishida M, Honda A, Ito Y. Transient receptor potential channels in cardiovascular function and disease. Circ Res. 2006; 99:119–131. [PubMed: 16857972]
11. Liu D, Zhu Z, Tepel M. The role of transient receptor potential channels in metabolic syndrome. Hypertens Res. 2008; 31:1989–1995. [PubMed: 19098369]
12. Hao X, Chen J, Luo Z, He H, Yu H, Ma L, Ma S, Zhu T, Liu D, Zhu Z. TRPV1 activation prevents high-salt diet-induced nocturnal hypertension in mice. Pflug Arch. 2011; 461:345–353.
13. Villamena, FA. Molecular Basis of Oxidative Stress. John Wiley & Sons, Inc; 2013. Chemistry of reactive species; p. 1-48.
14. Ayala A, Muñoz MF, Argüelles S. Lipid peroxidation: production, metabolism, and signaling mechanisms of malondialdehyde and 4-hydroxy-2-nonenal. Oxid Med Cell Longev. 2014; 2014:360438. [PubMed: 24999379]
15. Benedetti A, Comporti M, Esterbauer H. Identification of 4-hydroxynonenal as a cytotoxic product originating from the peroxidation of liver microsomal lipids. Biochim Et Biophys Acta (BBA) – Lipids Lipid Metab. 1980; 620:281–296.
16. Esterbauer H, Fau Schaur Rj, Zollner H, Zollner H. Chemistry and Biochemistry of 4-Hydroxynonenal, Malonaldehyde and Related Aldehydes. 1991
17. Nadkarni DV, Sayre LM. Structural Definition of Early Lysine and Histidine Adduction Chemistry of 4-Hydroxynonenal. 1995
18. Pryor WA, Porter NA. Suggested Mechanisms for the Production of 4-Hydroxy-2-Nonenal from the Autoxidation Of Polyunsaturated Fatty Acids. 1990
19. Bennaars-Eiden A, Higgins L, Hertzel AV, Kapphahn RJ, Ferrington DA, Bernlohr DA. Covalent modification of epithelial fatty acid-binding protein by 4-hydroxynonenal in vitro and in vivo: evidence for a role in antioxidant biology. J Biol Chem. 2002; 277:50693–50702. [PubMed: 12386159]
20. Wang Z, Dou X, Gu D, Shen C, Yao T, Nguyen V, Braunschweig C, Song Z. 4-Hydroxynonenal differentially regulates adiponectin gene expression and secretion via activating PPARγ and

accelerating ubiquitin–proteasome degradation. Mol Cell Endocrinol. 2012; 349:222–231. [PubMed: 22085560]

21. Pillon NJ, Croze ML, Vella RE, Soulère L, Lagarde M, Soulage CO. The lipid peroxidation by-product 4-hydroxy-2-nonenal (4-HNE) induces insulin resistance in skeletal muscle through both carbonyl and oxidative stress. Endocrinology. 2012; 153:2099–2111. [PubMed: 22396448]
22. Zhang H, Forman HJ. 4-Hydroxynonenal activates Src through a non-canonical pathway that involves EGFR/PTP1B. Free Radic Biol Med. 2015; 89:701–707. [PubMed: 26453921]
23. Chuang HH, Lin S. Oxidative challenges sensitize the capsaicin receptor by covalent cysteine modification. Proc Natl Acad Sci USA. 2009; 106:20097–20102. [PubMed: 19897733]
24. Andersson DA, Gentry C, Moss S, Bevan S. Transient receptor potential A1 Is a sensory receptor for multiple products of oxidative stress. J Neurosci. 2008; 28:2485–2494. [PubMed: 18322093]
25. DelloStritto DJ, Connell PJ, Dick GM, Fancher IS, Klarich B, Fahmy JN, Kang PT, Chen Y-R, Damron DS, Thodeti CK, Bratz IN. Differential regulation of TRPV1 channels by H2O2: implications for diabetic microvascular dysfunction. Basic Res Cardiol. 2016; 111:1–16. [PubMed: 26597728]
26. Krieger E, Koraimann G, Vriend G. Increasing the precision of comparative models with YASARA NOVA—a self-parameterizing force field. Proteins: Struct Funct Bioinform. 2002; 47:393–402.
27. Moiseenkova-Bell VY, Stanciu LA, Serysheva II, Tobe BJ, Wensel TG. Structure of TRPV1 channel revealed by electron cryomicroscopy. Proc Natl Acad Sci USA. 2008; 105:7451–7455. [PubMed: 18490661]
28. Trott O, Olson AJ. AutoDock vina: improving the speed and accuracy of docking with a new scoring function, efficient optimization, and multithreading. J Comput Chem. 2010; 31:455–461. [PubMed: 19499576]
29. Pillon, NJ., Soulage, CO. Lipid Peroxidation by-Products and the Metabolic Syndrome. 2012.
30. Zhang H, Wickley PJ, Sinha S, Bratz IN, Damron DS. Propofol restores transient receptor potential vanilloid receptor subtype-1 sensitivity via activation of transient receptor potential ankyrin receptor subtype-1 in sensory neurons. Anesthesiology. 2011; 114:1169–1179. [PubMed: 21364461]
31. Nakayama M, Inoguchi T, Sonta T, Maeda Y, Sasaki S, Sawada F, Tsubouchi H, Sonoda N, Kobayashi K, Sumimoto H, Nawata H. Increased expression of NAD(P)H oxidase in islets of animal models of Type 2 diabetes and its improvement by an AT1 receptor antagonist. Biochem Biophys Res Commun. 2005; 332:927–933. [PubMed: 15922295]
32. Jaganjac M, Tirosh O, Cohen G, Sasson S, Zarkovic N. Reactive aldehydes – second messengers of free radicals in diabetes mellitus. Free Radic Res. 2013; 47:39–48. [PubMed: 23521622]
33. Mali VR, Palaniyandi SS. Regulation and therapeutic strategies of 4-hydroxy-2-nonenal metabolism in heart disease. Free Radic Res. 2014; 48:251–263. [PubMed: 24237196]
34. Chapple SJ, Cheng X, Mann GE. Effects of 4-hydroxynonenal on vascular endothelial and smooth muscle cell redox signaling and function in health and disease. Redox Biol. 2013; 1:319–331. [PubMed: 24024167]
35. Dolinsky VW, Chan AY, Robillard Frayne I, Light PE, Des Rosiers C, Dyck JR. Resveratrol prevents the prohypertrophic effects of oxidative stress on LKB1. Circulation. 2009; 119:1643–1652. [PubMed: 19289642]
36. Chung HS, Wang SB, Venkatraman V, Murray CI, Van Eyk JE. Cysteine oxidative posttranslational modifications: emerging regulation in the cardiovascular system. Circ Res. 2013; 112:382–392. [PubMed: 23329793]
37. Poli G, Schaur RJ, Siems WG, Leonarduzzi G. 4-Hydroxynonenal: a membrane lipid oxidation product of medicinal interest. Med Res Rev. 2008; 28:569–631. [PubMed: 18058921]
38. Usatyuk PV, Parinandi NL, Natarajan V. Redox regulation of 4-hydroxy-2-nonenal-mediated endothelial barrier dysfunction by focal adhesion, adherens, and tight junction proteins. J Biol Chem. 2006; 281:35554–35566. [PubMed: 16982627]
39. Hyun DH. Effect of the overexpression of mutant ubiquitin (K48R) on the cellular response induced by 4-hydroxy-2,3-trans-nonenal, an end-product of lipid peroxidation. Neurosci Lett. 2010; 477:115–120. [PubMed: 20433899]

40. Chapple SJ, Cheng X, Mann GE. Effects of 4-hydroxynonenal on vascular endothelial and smooth muscle cell redox signaling and function in health and disease. Redox Biol. 2013; 1:319–331. [PubMed: 24024167]
41. Usatyuk PV, Natarajan V. Role of mitogen-activated protein kinases in 4-hydroxy-2-nonenal-induced actin remodeling and barrier function in endothelial cells. J Biol Chem. 2004; 279:11789–11797. [PubMed: 14699126]
42. Trevisani M, Siemens J, Materazzi S, Bautista DM, Nassini R, Campi B, Imamachi N, Andrè E, Patacchini R, Cottrell GS, Gatti R, Basbaum AI, Bunnett NW, Julius D, Geppetti P. 4-Hydroxynonenal, an endogenous aldehyde, causes pain and neurogenic inflammation through activation of the irritant receptor TRPA1. Proc Natl Acad Sci USA. 2007; 104:13519–13524. [PubMed: 17684094]
43. Chuang, H-h, Lin, S. Oxidative challenges sensitize the capsaicin receptor by covalent cysteine modification. Proc Natl Acad Sci USA. 2009; 106:20097–20102. [PubMed: 19897733]
44. Susankova K, Tousova K, Vyklicky L, Teisinger J, Vlachova V. Reducing and oxidizing agents sensitize heat-activated vanilloid receptor (TRPV1) current. Mol Pharmacol. 2006; 70:383–394. [PubMed: 16614139]
45. Pope AJ, Druhan L, Guzman JE, Forbes SP, Murugesan V, Lu D, Xia Y, Chicoine LG, Parinandi NL, Cardounel AJ. Role of DDAH-1 in lipid peroxidation product-mediated inhibition of endothelial NO generation. Am J Physiol – Cell Physiol. 2007; 293:C1679–C1686. [PubMed: 17881609]
46. Bernatchez PN, Bauer PM, Yu J, Prendergast JS, He P, Sessa WC. Dissecting the molecular control of endothelial NO synthase by caveolin-1 using cell-permeable peptides. Proc Natl Acad Sci USA. 2005; 102:761–766. [PubMed: 15637154]
47. Kraehling JR, Hao Z, Lee MY, Vinyard DJ, Velazquez H, Liu X, Stan RV, Brudvig GW, Sessa WC. Uncoupling caveolae from intracellular signaling in vivo. Circ Res. 2016; 118:48–55. [PubMed: 26602865]
48. Ching LC, Kou YR, Shyue SK, Su KH, Wei J, Cheng LC, Yu YB, Pan CC, Lee TS. Molecular mechanisms of activation of endothelial nitric oxide synthase mediated by transient receptor potential vanilloid type 1. Cardiovasc Res. 2011; 91:492–501. [PubMed: 21493704]
49. Ching LC, Chen CY, Su KH, Hou HH, Shyue SK, Kou YR, Lee TS. Implication of AMP-activated protein kinase in transient receptor potential vanilloid type 1-mediated activation of endothelial nitric oxide synthase. Mol Med. 2012; 18:805–815. [PubMed: 22451268]
50. Ching LC, Zhao JF, Su KH, Shyue SK, Hsu CP, Lu TM, Lin SJ, Lee TS. Activation of transient receptor potential vanilloid 1 decreases endothelial nitric oxide synthase phosphorylation at Thr497 by protein phosphatase 2B-dependent dephosphorylation of protein kinase C. Acta Physiol. 2013; 209:124–135.
51. Cohen G, Riahi Y, Sunda V, Deplano S, Chatgilialoglu C, Ferreri C, Kaiser N, Sasson S. Signaling properties of 4-hydroxyalkenals formed by lipid peroxidation in diabetes. Free Radic Biol Med. 2013; 65:978–987. [PubMed: 23973638]
52. Wang S, Chuang HH. C-terminal dimerization activates the nociceptive transduction channel transient receptor potential vanilloid 1. J Biol Chem. 2011; 286:40601–40607. [PubMed: 21926175]
53. Ogawa N, Kurokawa T, Fujiwara K, Polat OK, Badr H, Takahashi N, Mori Y. Functional and structural divergence in human TRPV1 channel subunits by oxidative cysteine modification. J Biol Chem. 2016; 291:4197–4210. [PubMed: 26702055]

Appendix A. Supplementary material

Supplementary data associated with this article can be found in the online version at http://dx.doi.org/10.1016/j.freeradbiomed.2016.09.021.

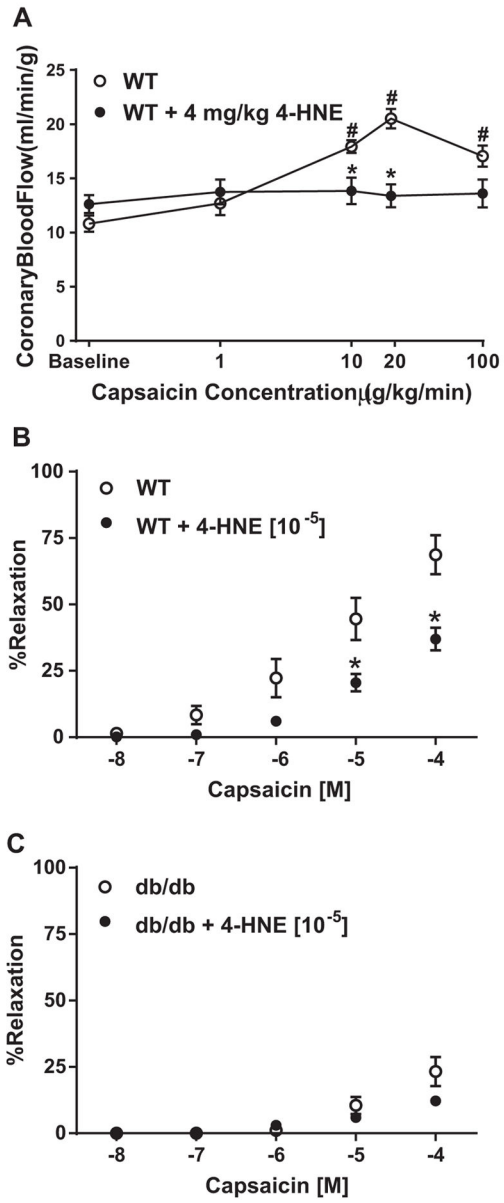

Fig. 1.

4-HNE effects on TRPV1 mediated microvascular signaling. A) Contrast echocardiography measurements of capsaicin-mediated changes in coronary blood flow in WT mice (n=7) and following 4-HNE infusion (n=6; 4 mg/kg). B) TRPV1-dependent coronary microvessel relaxation in the presence and absence of 4-HNE (10 μM) (n=7 vessels). C) db/db coronary microvessel relaxation to increasing concentrations of capsaicin in the presence and absence of 4-HNE (10 μM) (n=6 vessels) *P < 0.05 vs. WT analyzed by two-way ANOVA.

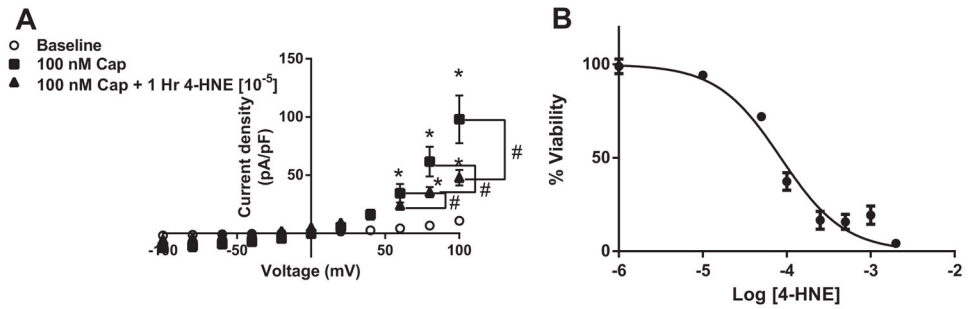

Fig. 2.

4-HNE effects on TRPV1 activation and survival. A) Summary of current-voltage (I–V) data using whole cell patch-clamp electrophysiology, examining effects of capsaicin-induced TRPV1 currents with or without 1-hr pre-treatment with 10 μM 4-HNE in transiently transfected HEK cells with WT-rTRPV1 (n=9 cells, capsaicin; n=9 cells, 4-HNE). B) HEK cells were investigated for cell survival in the presence of increasing 4-HNE concentrations for 1-h. HEK cells demonstrated an LC_{50} of 84.9 μM (R^2=0.861) *P < 0.05 vs. WT analyzed by two-way ANOVA (Panel A and B). *P < 0.05 vs. baseline analyzed by two-way ANOVA; $^{\#}$P < 0.05 vs. control analyzed by two-way ANOVA.

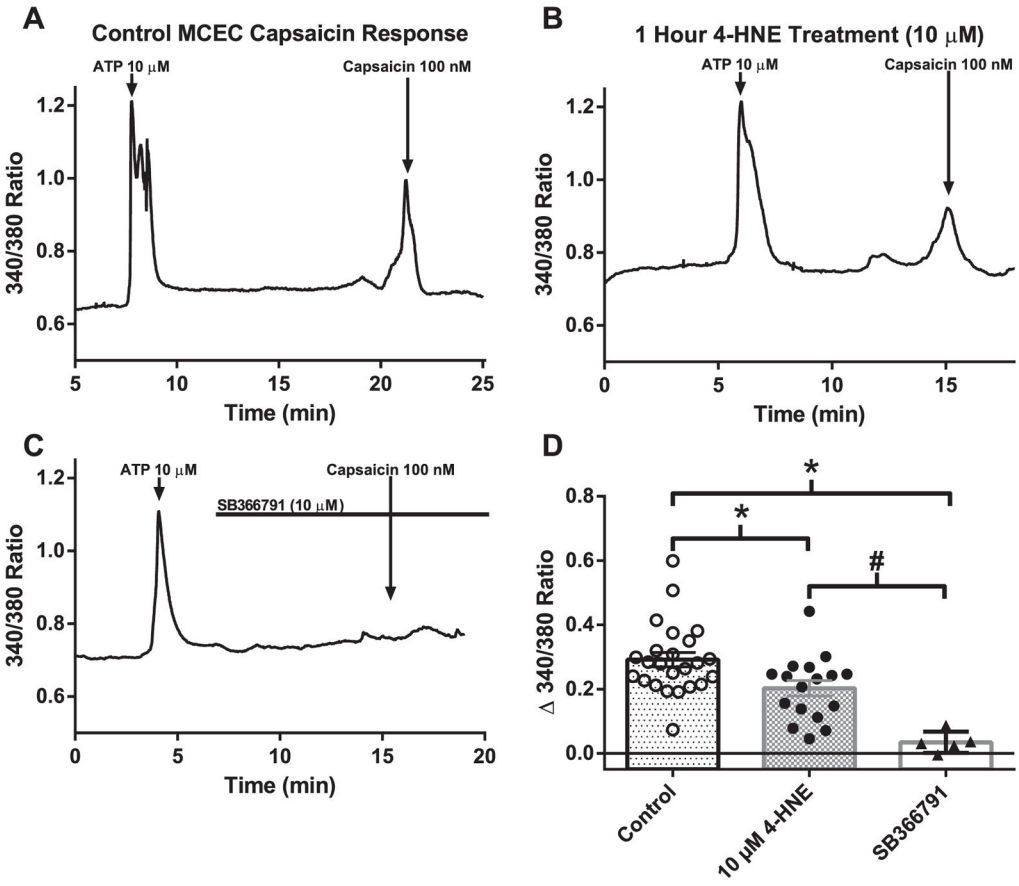

Fig. 3.

Effects of 4-HNE on native TRPV1 Ca^{2+} influx. Representative traces of capsaicin-mediated Ca^{2+} influx in MCECs to 100 nM capsaicin (A), to 100 nM capsaicin+10 μM 4-HNE (1-h pretreatment) (B) and to capsaicin+SB366791 (TRPV1 inhibitor;10 μM) (C). D) Quantification of peak Ca^{2+} compared to baseline in control and 4-HNE treated MCECs and SB366791 treated cells (n=24 cells, baseline; n=17 cells, 4-HNE; n=5 cells, SB366791). *P < 0.05 vs. control analyzed by one-way ANOVA; #P < 0.05 vs. 4-HNE treatment analyzed by one-way ANOVA.

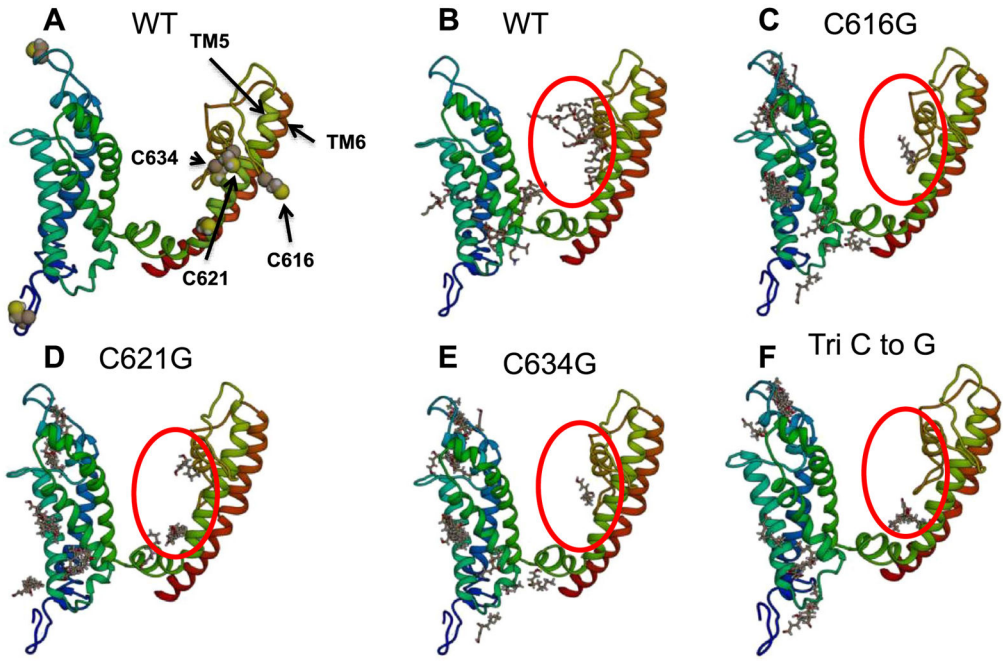

Fig. 4.

Computational modeling of transmembrane region of TRPV1 and 4-HNE-associated binding sites. A) Utilizing the computational program, YASARA 14.7.17, the transmembrane region of TRPV1 was constructed. B) The binding algorithm Autodock VINA predicting possible 4-HNE interaction in WT-TRPV1 and decreased interaction in the following mutant TRPV1 constructs C) C616G-TRPV1, D) C621G-TRPV1, E) C634G-TRPV1 and F) Tri C to G-TRPV1.

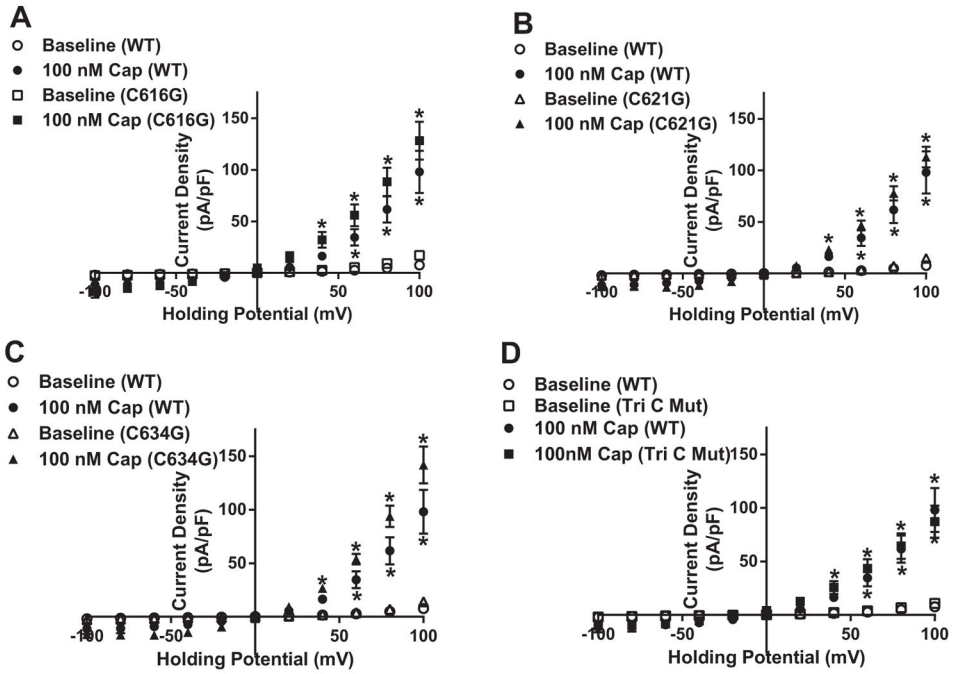

Fig. 5.

Functionality of mutant TRPV1 constructs. Summary I–V plots of capsaicin-dependent currents using whole cell electrophysiology in transiently transfected HEK cells in each mutant construct A) C616G-TRPV1 (n=8 cells, capsaicin), B) C621G-TRPV1 (n=13 cells, capsaicin), C) C634G-TRPV1 (n=11 cells, capsaicin) and D) Tri C to G-TRPV1 (n=8 cells, capsaicin) compared to WT-TRPV1 (n=9 cells, capsaicin). *P < 0.05 vs. baseline analyzed by two-way ANOVA.

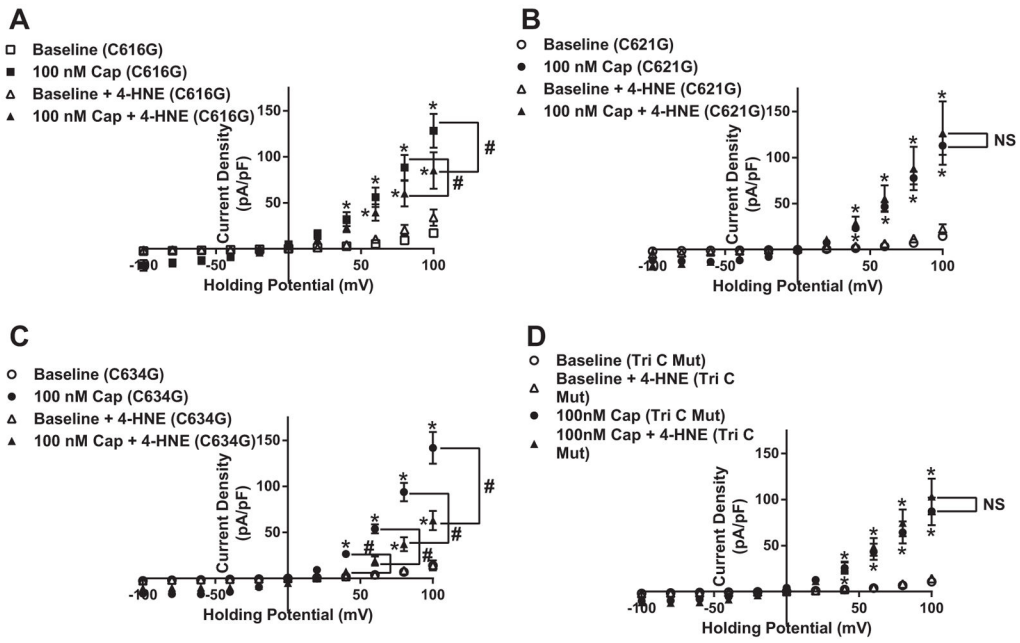

Fig. 6.

C621G mutation rescue 4-HNE-associated decreases in capsaicin-dependent TRPV1-mediated current. Summary I–V plots of capsaicin-dependent currents using whole cell electrophysiology in transiently transfected HEK cells in each mutant construct A) C616G-TRPV1 (n=8 cells, capsaicin; n=9 cells, 4-HNE), B) C621G-TRPV1 (n=13 cells, capsaicin; n=6 cells, 4-HNE), C) C634G-TRPV1 (n=11 cells, capsaicin; n=7 cells, 4-HNE) and D) Tri C to G-TRPV1 (n=8 cells, capsaicin; n=10 cells, 4-HNE) in the presence and absence of 10 μM 4-HNE. *P < 0.05 vs. baseline analyzed by two-way ANOVA; #P < 0.05 vs. control analyzed by two-way ANOVA.

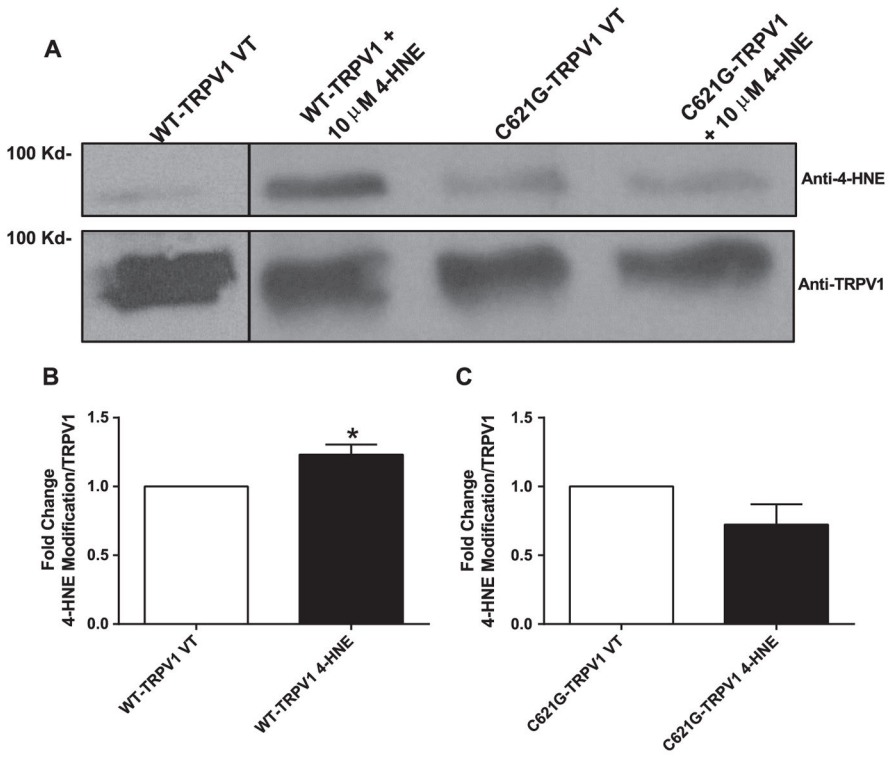

Fig. 7.

Mutant TRPV1 construct C621G prevents 4-HNE-mediated TRPV1 PTM. A) Representative blot of 6x His-tag pull down of WT and C621 TRPV1 following 1-h treatment of 10 μM 4-HNE. Subsequent samples were probed for both 4-HNE and TRPV1. B) Quantification of 4-HNE-mediated TRPV1 PTM in WT-TRPV1 treated cells (n=4 separate experiments). C) Quantification of 4-HNE-mediated TRPV1 PTM in C621G-TRPV1 treated cells (n=4 separate experiments). *P < 0.05 vs. vehicle treated analyzed by student's *t*-test.

Table 1

Heart rate and blood pressure measurements. Summary of HR and BP in WT mice in the presence and absence of 4-HNE.

	WT	WT	WT (4-HNE)	WT (4-HNE)
[Capsaicin] (μg/kg)	**Blood pressure**	**Heart rate**	**Blood pressure**	**Heart rate**
Baseline	72.2 ± 5.6	517 ± 26	65.9 ± 6.6	493 ± 20
1	75.0 ± 5.3	499 ± 24	66.7 ± 6.6	500 ± 20
10	77.1 ± 5.4	479 ± 24	66.0 ± 6.2	494 ± 20
20	81.5 ± 5.4	480 ± 20	70.1 ± 3.4	497 ± 19
100	88.2 ± 6.5	501 ± 12	83.9 ± 5.2	492 ± 24